JCI The Journal of Clinical Investigation

Bone marrow cells recruited through the neuropilin-1 receptor promote arterial formation at the sites of adult neoangiogenesis in mice

Serena Zacchigna, … , Gianfranco Sinagra, Mauro Giacca

J Clin Invest. 2008;118(6):2062-2075. https://doi.org/10.1172/JCI32832.

Research Article **Vascular biology**

Experimental and clinical evidence indicate that bone marrow cells participate in the process of new blood vessel formation. However, the molecular mechanisms underlying their recruitment and their exact role are still elusive. Here, we show that bone marrow cells are recruited to the sites of neoangiogenesis through the neuropilin-1 (NP-1) receptor and that they are essential for the maturation of the activated endothelium and the formation of arteries in mice. By exploiting adeno-associated virus vector–mediated, long-term in vivo gene expression, we show that the 165-aa isoform of VEGF, which both activates the endothelium and recruits NP-1$^+$ myeloid cells, is a powerful arteriogenic agent. In contrast, neither the shortest $VEGF_{121}$ isoform, which does not bind NP-1 and thus does not recruit bone marrow cells, nor semaphorin 3A, which attracts cells but inhibits endothelial activation, are capable of sustaining arterial formation. Bone marrow myeloid cells are not arteriogenic per se nor are they directly incorporated in the newly formed vasculature, but they contribute to arterial formation through a paracrine effect ensuing in the activation and proliferation of tissue-resident smooth muscle cells.

Bone marrow cells recruited through the neuropilin-1 receptor promote arterial formation at the sites of adult neoangiogenesis in mice

Serena Zacchigna,[1] Lucia Pattarini,[1] Lorena Zentilin,[1] Silvia Moimas,[1] Alessandro Carrer,[1] Milena Sinigaglia,[1] Nikola Arsic,[1] Sabrina Tafuro,[1] Gianfranco Sinagra,[2] and Mauro Giacca[1]

[1]Molecular Medicine Laboratory, International Centre for Genetic Engineering and Biotechnology (ICGEB), Trieste, Italy.
[2]Cardiovascular Department, "Ospedali Riuniti" and University of Trieste, Trieste, Italy.

Experimental and clinical evidence indicate that bone marrow cells participate in the process of new blood vessel formation. However, the molecular mechanisms underlying their recruitment and their exact role are still elusive. Here, we show that bone marrow cells are recruited to the sites of neoangiogenesis through the neuropilin-1 (NP-1) receptor and that they are essential for the maturation of the activated endothelium and the formation of arteries in mice. By exploiting adeno-associated virus vector–mediated, long-term in vivo gene expression, we show that the 165-aa isoform of VEGF, which both activates the endothelium and recruits NP-1$^+$ myeloid cells, is a powerful arteriogenic agent. In contrast, neither the shortest $VEGF_{121}$ isoform, which does not bind NP-1 and thus does not recruit bone marrow cells, nor semaphorin 3A, which attracts cells but inhibits endothelial activation, are capable of sustaining arterial formation. Bone marrow myeloid cells are not arteriogenic per se nor are they directly incorporated in the newly formed vasculature, but they contribute to arterial formation through a paracrine effect ensuing in the activation and proliferation of tissue-resident smooth muscle cells.

Introduction

New blood vessel formation during postnatal life has been traditionally considered to arise through angiogenesis, a complex process essentially entailing the sprouting of new capillaries from preexisting vessels to form an immature vascular network that subsequently undergoes functional remodeling (1, 2). The different members of the VEGF family have long been recognized as playing an essential role in this process. Five isoforms of VEGF-A (herein VEGF for brevity) have been identified in humans: $VEGF_{121}$, $VEGF_{145}$, $VEGF_{165}$, $VEGF_{189}$, and $VEGF_{206}$, generated by alternative splicing of a primary *VEGF* gene transcript (all isoforms are 1 amino acid shorter in mice). $VEGF_{165}$ is the most abundant and biologically active isoform, being able to bind Flk-1 (VEGFR-2) and Flt-1 (VEGFR-1), 2 receptors expressed by most vascular endothelial cells. Of interest, the different VEGF isoforms do not appear equivalent in function. In particular, knockout mice expressing only $VEGF_{164}$ are normal, while those expressing only $VEGF_{120}$ exhibit specific defects in retinal, coronary, and renal arterial development (3–5). This observation suggests that the $VEGF_{164}$ isoform might be specifically involved in arterial specification and periendothelial cell recruitment.

More recently, an additional, nontyrosine kinase receptor for $VEGF_{165}$ called *neuropilin-1* (NP-1) has been identified, able to significantly enhance the affinity of $VEGF_{165}$ to Flk-1 (6, 7). Notably, NP-1 specifically interacts with $VEGF_{165}$ but not with $VEGF_{121}$, which lacks exon 7. The functional consequence of this dissimilar NP-1–binding capacity has been largely overlooked so far (8). NP-1 was originally discovered as the main receptor for semaphorin 3a (Sema3A), a member of the semaphorin family that provides repulsive guiding cues to axonal growth cones in the developing nervous system (9). Despite a growing body of evidence indicating that NP-1 also plays an essential role in normal vascular development (10, 11), the underlying mechanisms and the in vivo function of this receptor still remain poorly understood.

Over the last several years, results from different experimental settings have indicated that circulating cells derived from the BM actively contribute to new blood vessel formation during both normal and tumor neovascularization. Different studies have highlighted the existence of a population of endothelial progenitor cells that eventually become incorporated within the newly formed vasculature through a differentiation process resembling embryonic vasculogenesis (12, 13). The existence of endothelial progenitor cells has engendered much excitement and has prompted a rapid transposition of this concept to the clinics. The actual relevance of this process, however, has been recently questioned by a series of experimental studies (14, 15) as well as by the results of clinical trials entailing the injection of total BM sites into ischemic tissues (see ref. 16 and citations therein).

A set of BM-derived cells that home to the sites of adult neovascularization bear markers of myeloid origin and have been alternatively considered as tissue-resident macrophages (17), circulating monocytes (18), or more generically, mononuclear cells (19) or inflammatory cells (20). Indeed, we and others have observed that in both conditional transgenic animals (21, 22) and animals injected with viral vectors (23) or implanted with engineered cells (24), the sites of prolonged $VEGF_{165}$ expression become infiltrated by a large number of cells bearing myeloid markers.

Nonstandard abbreviations used: AAV, adeno-associated virus; AP, alkaline phosphatase; NP-1, neuropilin-1; rh, recombinant human; SDF-1, stromal-derived factor-1; Sema3A, semaphorin 3A.

Conflict of interest: The authors have declared that no conflict of interest exists.

Citation for this article: *J. Clin. Invest.* **118**:2062–2075 (2008). doi:10.1172/JCI32832.

Here, we tackle the issue of understanding the role of the BM-derived mononuclear cells in the process of new blood vessel formation by exploiting an in vivo gene transfer approach based on the use of vectors derived from the adeno-associated virus (AAV). These vectors represent excellent tools for in vivo investigation, since they efficiently transduce postmitotic tissues in vivo and sustain transgene expression for prolonged periods of time in the absence of any inflammatory or immune response. By taking advantage of these properties, we determined the effect of the long-term expression of $VEGF_{165}$, $VEGF_{121}$, and Sema3A in adult skeletal muscle. For what we believe is the first time, we provide evidence that the recruitment of myeloid cells of BM origin to the sites of neoangiogenesis occurs through the NP-1 receptor and is a peculiar feature of $VEGF_{165}$. We demonstrate that these BM cells are essential for the process of arterial formation, since they provide chemoattraction for resident SMCs that contribute to proper vessel maturation. These results are relevant for the understanding of the process leading to functional new blood vessel formation in adult organisms, with particular reference to several gene therapy clinical trials aimed at inducing therapeutic angiogenesis.

Results

Different angiogenic phenotypes induced by the prolonged expression of VEGF isoforms and of Sema3A. In keeping with our previous observations (23, 25–27), the prolonged expression of $VEGF_{165}$ in normoperfused rodent skeletal muscle was found to induce a massive angiogenic response, which was mainly characterized by the formation of a large number of arterioles. These vessels had a 20–120–μm diameter and were provided with a thick layer of α-SMA– and NG2-positive cells (Figure 1A and references above). Of interest, the sites of VEGF-induced angiogenesis were always interspersed with a wide infiltration of mononuclear cells. We have previously shown that these infiltrating cells are of BM origin; in no case, however, were these cells found to directly differentiate into the α-SMA–positive cells covering the newly formed arterioles (see ref. 25 and Supplemental Figure 1; supplemental material available online with this article; doi:10.1172/JCI32832DS1). To our surprise, when a similar experiment was performed by the injection of an AAV vector expressing $VEGF_{121}$, no cellular infiltration was observed. Even more intriguingly, the absence of mononuclear cell infiltration was paralleled by a remarkably poor formation of arterioles (Figure 1A).

To quantify the effects of both VEGF isoforms in terms of capillary and artery formation, we performed CD31/α-SMA double immunofluorescence on muscle sections from mice injected with either AAV-$VEGF_{165}$ or AAV-$VEGF_{121}$ and quantified the relative areas occupied by cellular nuclei (DAPI staining), endothelial cells (CD31), and SMCs (α-SMA) at 1 month after transduction. Both VEGF isoforms stimulated the proliferation of endothelial cells to a similar extent; however, a specific increase in the total number of cells as well as in the number of α-SMA–positive vessels was only evident in muscles expressing $VEGF_{165}$ (Figure 1B).

Both $VEGF_{121}$ and $VEGF_{165}$ bind the canonical VEGF receptors (Flt-1 and Flk-1), whereas only $VEGF_{165}$ also interacts with the coreceptor NP-1, a specific receptor for Sema3A (Figure 1C) (28). We indeed found that the AAV-mediated delivery of Sema3A in the skeletal muscle promoted a massive cellular infiltration very similar to $VEGF_{165}$ (Figure 1D). In contrast with $VEGF_{165}$, however, no new blood vessels were detected in the muscles overexpressing Sema3A.

To further characterize the vascular network present in the muscles expressing $VEGF_{121}$, $VEGF_{165}$, or Sema3A, animals were perfused in vivo with a bolus of 0.2-μm diameter fluorescent microspheres in order to quantify the blood pool contained in the treated muscles by filling up the microcirculation. The results of this analysis indicated that both VEGF isoforms determined an almost 7-fold increase in vascular volume, while Sema3A had no effect (Supplemental Figure 2B) despite both transgenes being expressed at similar levels (Supplemental Figure 2A). Confocal microscopy 3D reconstructions of the microsphere distribution inside the microcirculation of animals treated with the different vectors and lectin staining of the perfused vessels are shown in Supplemental Figure 2, C and D–E, respectively.

In vivo inhibitory effect of Sema3A on $VEGF_{165}$-induced angiogenesis. We discovered that AAV-Sema3A when coinjected with AAV-$VEGF_{165}$ markedly suppressed $VEGF_{165}$-induced angiogenesis. At 1 month after injection of a 1:1 combination of the 2 vectors, a remarkable inhibition of $VEGF_{165}$-induced endothelial sprouting was evident (Figure 2A). This result is consistent with in vitro data showing that Sema3A counteracts endothelial cell activation by competing with $VEGF_{165}$ (6). Most notably, in a time-course experiment following injection of AAV-$VEGF_{165}$, AAV-Sema3A, or both, the formation of new α-SMA–positive arterioles induced by $VEGF_{165}$ at 1 and 3 months after injection was completely suppressed by Sema3A (Figure 2B). The extent of cellular infiltration was similar at the earlier time points (up to 14 days) for all 3 treatments; at 1 and 3 months after injection, however, the number of infiltrating cells remained substantially unchanged or increased in the samples expressing Sema3A (either alone or in combination with $VEGF_{165}$), while it was remarkably reduced with $VEGF_{165}$ alone. A dose-response analysis of the antiangiogenic effect of AAV-Sema3A is shown in Supplemental Figure 3.

The histological evidence that Sema3A exerts a potent inhibitory effect on neoangiogenesis was also reflected by the quenching of the $VEGF_{165}$-induced increase in vascular volume at 1 month after injection and by its complete abrogation at 3 months, as concluded after the injection of fluorescent microspheres (Figure 2C).

To further understand whether the antiangiogenic effect of Sema3A was exclusively due to competition with $VEGF_{165}$ for binding to NP-1 or might involve a direct negative effect of Sema3A on endothelial cells, we coinjected AAV-Sema3A with either AAV-$VEGF_{165}$ or AAV-$VEGF_{121}$ (since $VEGF_{121}$ does not bind NP-1, it should not compete with Sema3A). We observed that Sema3A was equally able to reduce the number of $CD31^+$ endothelial cells formed in response to both VEGF isoforms, suggesting a direct activity of Sema3A on the microvasculature (Figure 2D). Consistent with these findings, we also observed that several $CD31^+$ cells showed markers of apoptosis in muscles coexpressing $VEGF_{165}$ and Sema3A. The percentage of $CD31^+$ endothelial cells labeled by an anti-cleaved caspase-3 antibody was 6.8 ± 2.1 in muscles coinjected with AAV-$VEGF_{165}$ and AAV-Sema3A, whereas it was less than 1% in muscles injected with either vector alone; a representative picture of an AAV-$VEGF_{165}$ plus AAV-Sema3A–injected muscle after CD31/caspase-3 double labeling is shown in Figure 2E.

Characterization of the cells recruited to the muscles overexpressing $VEGF_{165}$ or Sema3A. Considering the unexpected property of both $VEGF_{165}$ and Sema3A to induce a massive cellular infiltration although apparently exerting opposite effects on vessel growth, we investigated to determine whether the cells recruited by Sema3A also derive from the BM, similar to what we have previously observed after $VEGF_{165}$ gene transfer (25). Unfractionated BM cells from male BALB/c donor mice were transplanted into lethally irradiated synge-

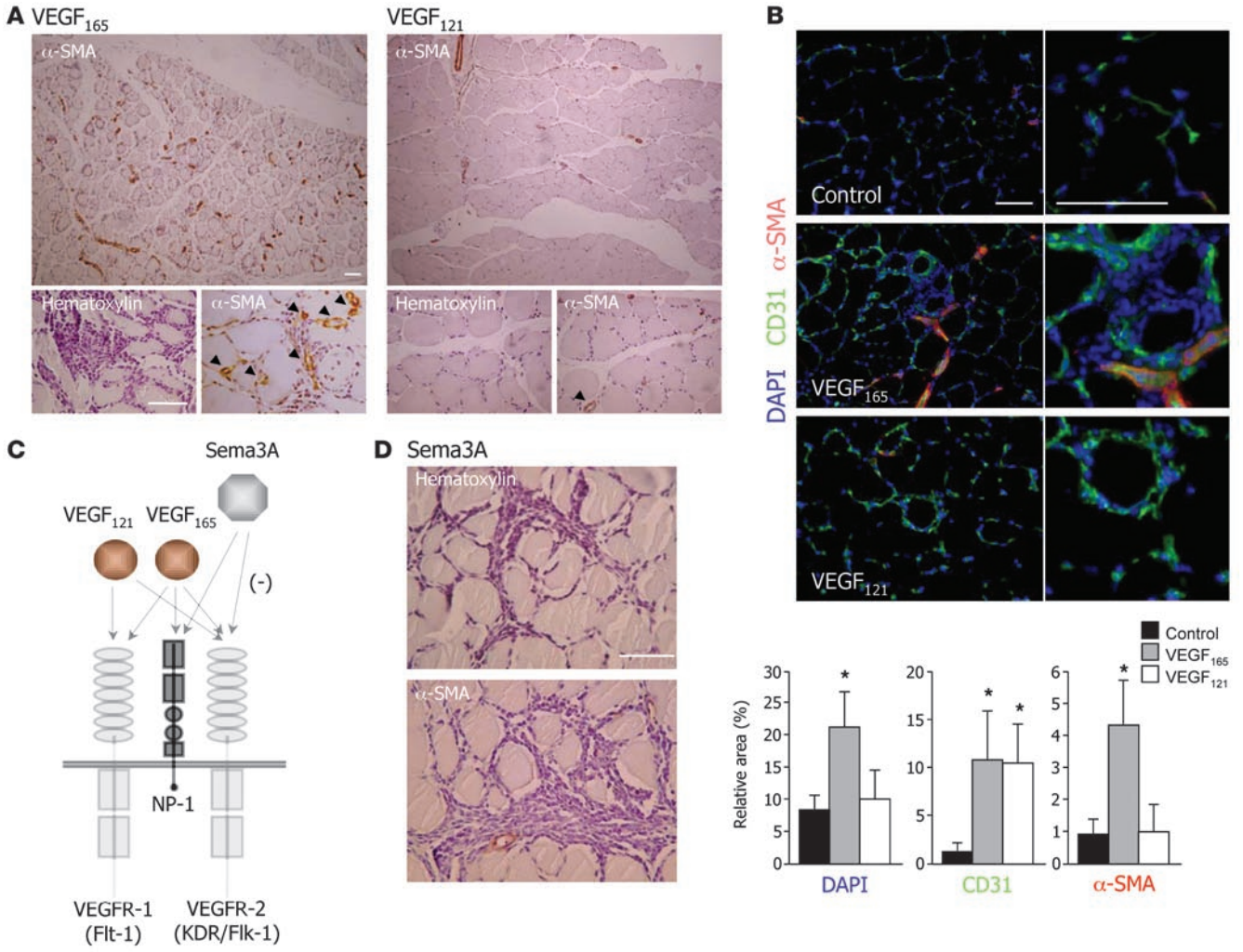

Figure 1

Differential effects of $VEGF_{165}$, $VEGF_{121}$, and Sema3A on angiogenesis. (**A**) α-SMA immunohistochemistry of muscle sections at 1 month after the injection of AAV-$VEGF_{121}$ or AAV-$VEGF_{165}$. While $VEGF_{165}$ induced the appearance of a striking number of arterioles interspersed within a massive infiltration of mononuclear cells, $VEGF_{121}$ was incapable of sustaining either effect. The lower panels show higher-magnification image to highlight the presence of cellular infiltration (hematoxylin staining on the left) and of arterial vessels (α-SMA staining on the right; arterioles indicated by black arrowheads), specifically in muscles expressing $VEGF_{165}$. Scale bars: 100 μm. (**B**) Comparison between $VEGF_{121}$- and $VEGF_{165}$-induced angiogenesis. While both VEGF isoforms induce endothelial cell proliferation to a similar extent (CD31 staining in green), only $VEGF_{165}$ expression results in a significant increase in the total number of cells (DAPI nuclear staining in blue) paralleled by the formation of new arteries (α-SMA staining in red). Histograms on the bottom show the quantification of the relative area occupied by cellular nuclei (DAPI), endothelial cells (CD31), or SMCs (α-SMA) in 20 independent sections for each treatment. Data are presented as means ± SD. *Statistical significance over control, AAV–LacZ-treated muscles ($P < 0.05$). Scale bars: 100 μm. (**C**) Schematic representation of the interactions between the 3 ligands ($VEGF_{165}$, $VEGF_{121}$, and Sema3A) and the 3 receptors (VEGFR-1/Flt-1, VEGFR-2/Flk-1, and NP-1) considered in this study. (**D**) Cellular infiltration induced by Sema3A in the absence of neoangiogenesis. The long-term overexpression of Sema3A induced the appearance of a mononuclear cell infiltration, very similar to the one observed in AAV-$VEGF_{165}$–treated muscles (hematoxylin staining in the upper panel). However, no new arteries could be detected in these muscles, as shown here by α-SMA immunohistochemistry (lower panel). Scale bar: 100 μm.

neic female recipients, thus creating Y-BALB/c chimeric mice. After successful engraftment (>90% of blood mononuclear cells of donor origin at 1 month after transplantation), these mice were injected with equal doses of either AAV-$VEGF_{165}$ or AAV-Sema3A ($n = 3$ per treatment). In situ hybridization to detect the Y chromosome using an FITC-labeled mouse DNA probe was performed at 1 month after vector injection. In our experimental settings, this procedure routinely detects approximately 80% of Y chromosome–positive cells when performed on tissues of male mice. In all transplanted, chimeric females injected with either vector, the majority of the infiltrating cells bore the Y chromosome (72% ± 7% and 78% ± 8% of Y chromosome–positive infiltrating cells in $VEGF_{165}$- and Sema3A-expressing muscles, respectively; Figure 3A). Moreover, as previously shown for $VEGF_{165}$ (25), these cells scored positive for the panleukocytic marker CD45 as well as for the myeloid marker CD11b (Figure 3B).

To begin to gain an understanding of which receptors might be involved in the recruitment of these cells, the cellular infiltrates formed in response to either AAV-$VEGF_{165}$ or AAV-Sema3A

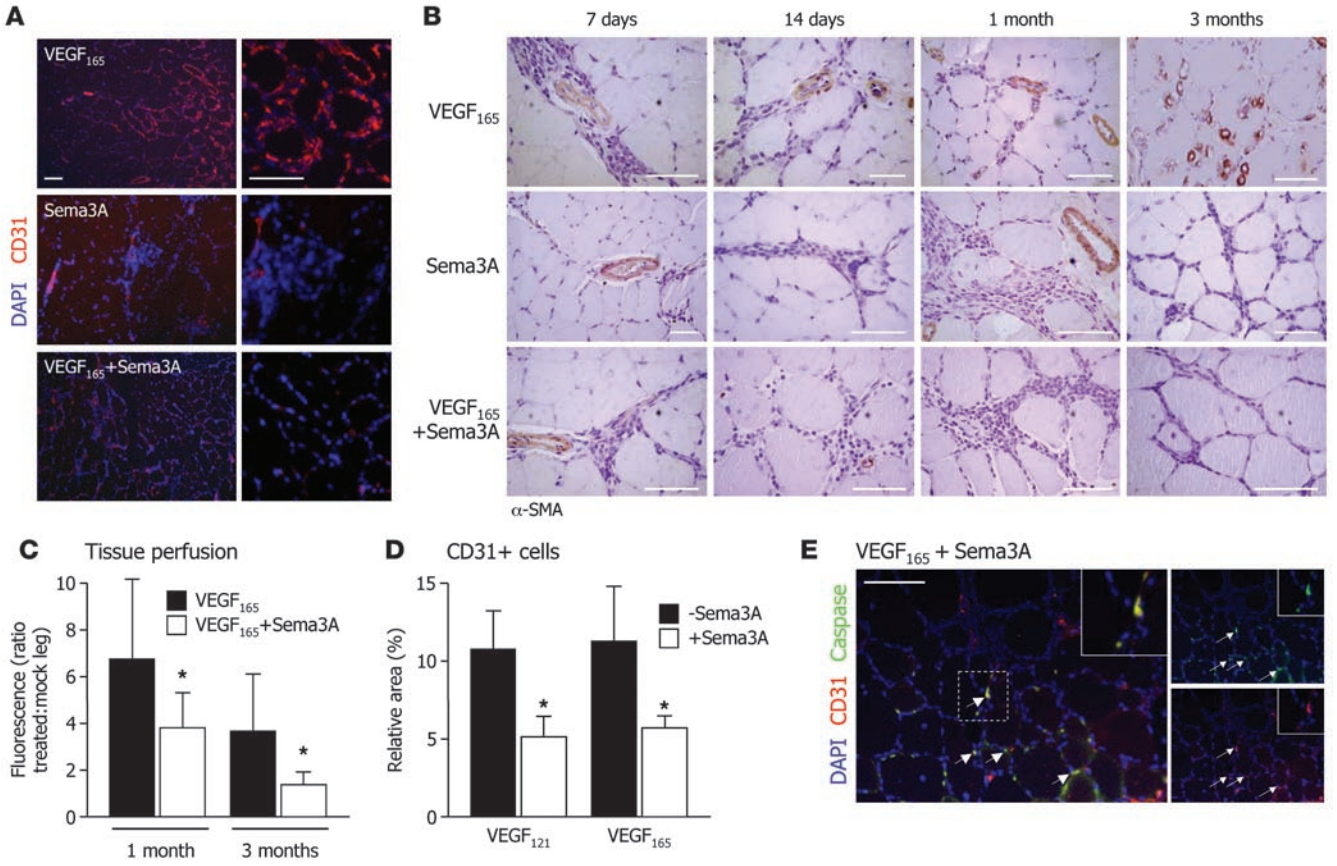

Figure 2

Inhibition of VEGF165-induced angiogenesis by Sema3A. (**A**) Staining with an α-CD31 antibody revealed massive angiogenic sprouting induced by $VEGF_{165}$ (upper panel), the absence of new capillary formation in Sema3A-expressing muscles (middle panel), and a potent effect of Sema3A in counteracting $VEGF_{165}$-induced angiogenesis (lower panel). Scale bars: 100 μm. (**B**) Immunohistochemistry using an anti–α-SMA antibody shows the progressive formation of arteries over time in muscles overexpressing $VEGF_{165}$ (upper panels), whereas new arteries were generated in response to Sema3A (middle panels). The combined expression of $VEGF_{165}$ with Sema3A resulted in an almost complete inhibition of the $VEGF_{165}$-induced angiogenic effect (lower panels). Scale bars: 100 μm. (**C**) The capacity of Sema3A to counteract the increase in vascular volume driven by $VEGF_{165}$ was assessed by fluorescent microspheres at both 1 and 3 months after vector delivery. Data are presented as a ratio between the emission value of the treated and the contralateral mock-treated muscle. Shown are means ± SD. $^*P < 0.05$. (**D**) The area occupied by endothelial cells, as measured by anti-CD31 fluorescent labeling, was quantified in muscles injected with AAV- $VEGF_{165}$ and AAV- $VEGF_{121}$, either alone or in combination with AAV-Sema3A. Shown are means ± SD. (**E**) The presence of apoptotic endothelial cells (white arrowheads) is shown by double labeling for the endothelial marker CD31 and for the apoptotic marker cleaved caspase-3 in muscles injected with AAV- $VEGF_{165}$ and AAV-Sema3A. Right panels show the blue/green (upper) and blue/red (lower) channels of the image. Insets show higher magnification. Scale bar: 100 μm.

were harvested by laser microdissection of muscle sections from the injected animals and the expression levels of the Flk-1, Flt-1, NP-1, and NP-2 receptors were measured by real-time PCR. The mononuclear cells found in the tissues expressing either $VEGF_{165}$ or Sema3A expressed abundant levels of NP-1 (Figure 3C). In contrast, Flk-1, Flt-1, and NP-2 were primarily detected in the muscles treated with AAV-$VEGF_{165}$, likely reflecting the presence of several activated endothelial cells in the microdissected samples. The expression levels of the 4 receptors were also quantified in primary $CD11b^+$ cells purified from the BM by the use of magnetic beads. The NP-1 receptor was also found abundantly expressed in these cells (Figure 3D). Finally, we further confirmed by double immunostaining that the vast majority of the $CD11b^+$ cells recruited to the muscles expressing either $VEGF_{165}$ or Sema3A were also positive for NP-1 (Figure 3E) but not for NP-2 (Figure 3F). Both NP-1 and NP-2 antibodies stained part of the microvasculature. Collectively, these results point toward an essential role of NP-1 in mediating the recruitment of BM cells induced by both $VEGF_{165}$ and Sema3A.

NP-1 is required for the recruitment of $CD11b^+$ cells by $VEGF_{165}$ and Sema3A. To further confirm that $VEGF_{165}$ and Sema3A share the property of being able to recruit myeloid cells, primary $CD11b^+$ cells were purified from the BM and tested for their ability to bind and migrate in response to recombinant human $VEGF_{121}$ (rhVEGF121), $VEGF_{165}$, or Sema3A. The results of the migration assay indicated that both $VEGF_{165}$ and Sema3A act as chemoattractants for $CD11b^+$ cells in a dose-dependent manner (Figure 4A). In contrast, a negligible number of cells migrated in response to $VEGF_{121}$. In a consistent manner, both $VEGF_{165}$ and Sema3A but not $VEGF_{121}$ expressed as recombinant proteins fused to alka-

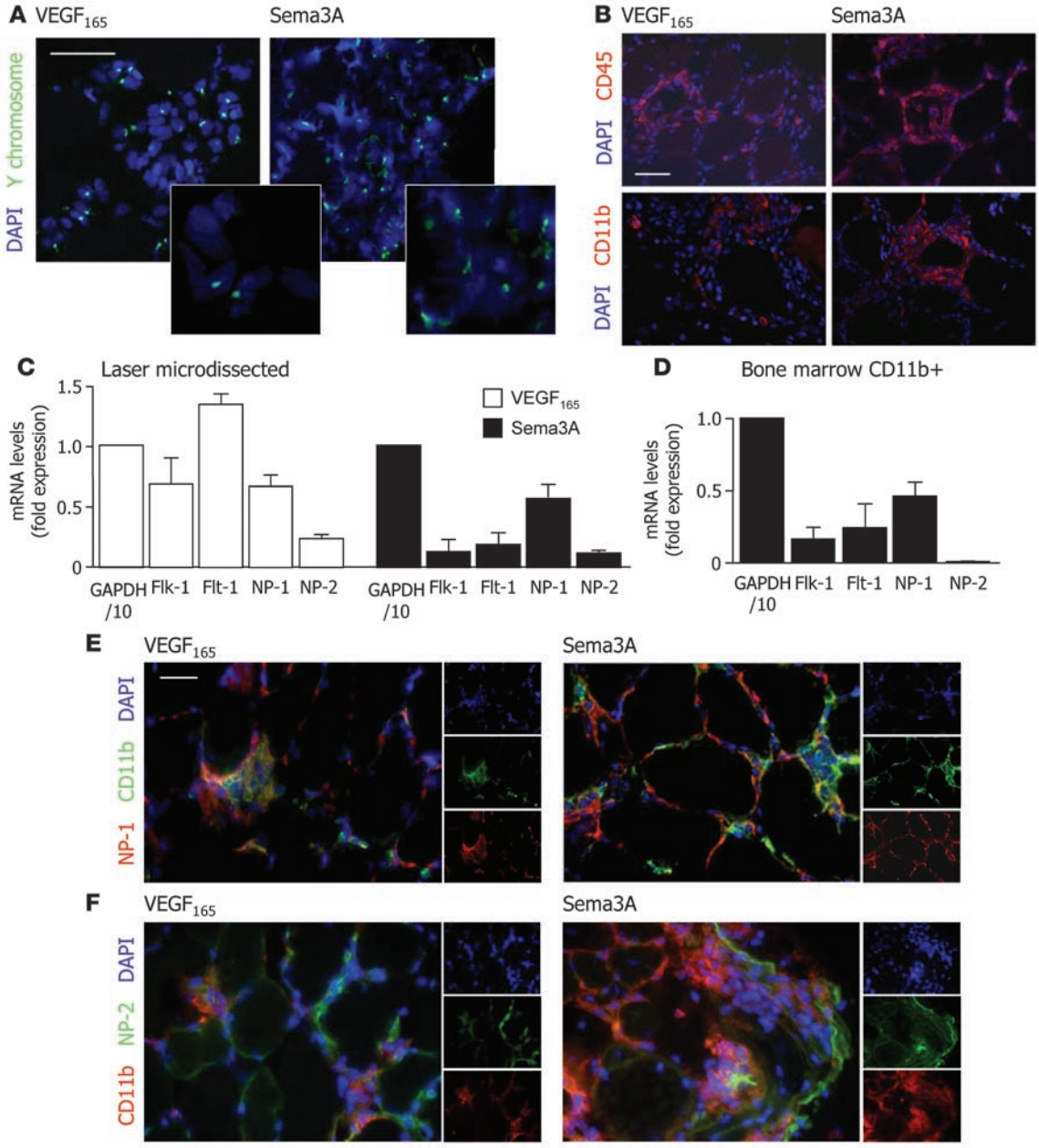

Figure 3

Recruitment of NP-1$^+$ myeloid cells by $VEGF_{165}$ and Sema3A. (**A**) The intramuscular injection of AAV-$VEGF_{165}$ or AAV-Sema3A in female mice transplanted with male BM determined a massive infiltration of Y chromosome–positive cells (shown by FISH as a green dot inside a DAPI-stained blue nucleus). Scale bar: 100 μm. (**B**) The vast majority (>80%) of the cells recruited by both $VEGF_{165}$ and Sema3A scored positive for the panleukocytic marker CD45 (left) as well as for the monocyte marker CD11b (right). Scale bar: 100 μm. (**C**) The cellular infiltrates from the muscles expressing either $VEGF_{165}$ or Sema3A were laser microdissected to determine the expression levels of Flk-1, Flt-1, NP-1, and NP-2 by real-time PCR (normalized to those of the housekeeping gene *GAPDH*). With the exception of NP-2, these receptors were abundantly expressed in $VEGF_{165}$-expressing muscles (white bars). In contrast, in muscles injected with AAV-Sema3A, NP-1 was the most abundantly expressed receptor (black bars). Shown are means ± SD of 3 independent quantifications. (**D**) The same quantifications described in **C** were performed on primary CD11b$^+$ cells purified from the BM. Shown are means ± SD of 3 independent quantifications. (**E**) The majority of the cells recruited by both $VEGF_{165}$ and Sema3A were colabeled by antibodies against CD11b (green) and NP-1 (red). NP-1 expression was also detected in the microvasculature (25). Scale bar: 100 μm. (**F**) Infiltrating CD11b$^+$ cells from $VEGF_{165}$- and Sema3A-transduced muscles were stained with antibodies against CD11b$^+$ (red) and NP-2 (green). The majority of cells scored negative for NP-2, which was expressed by some vessels.

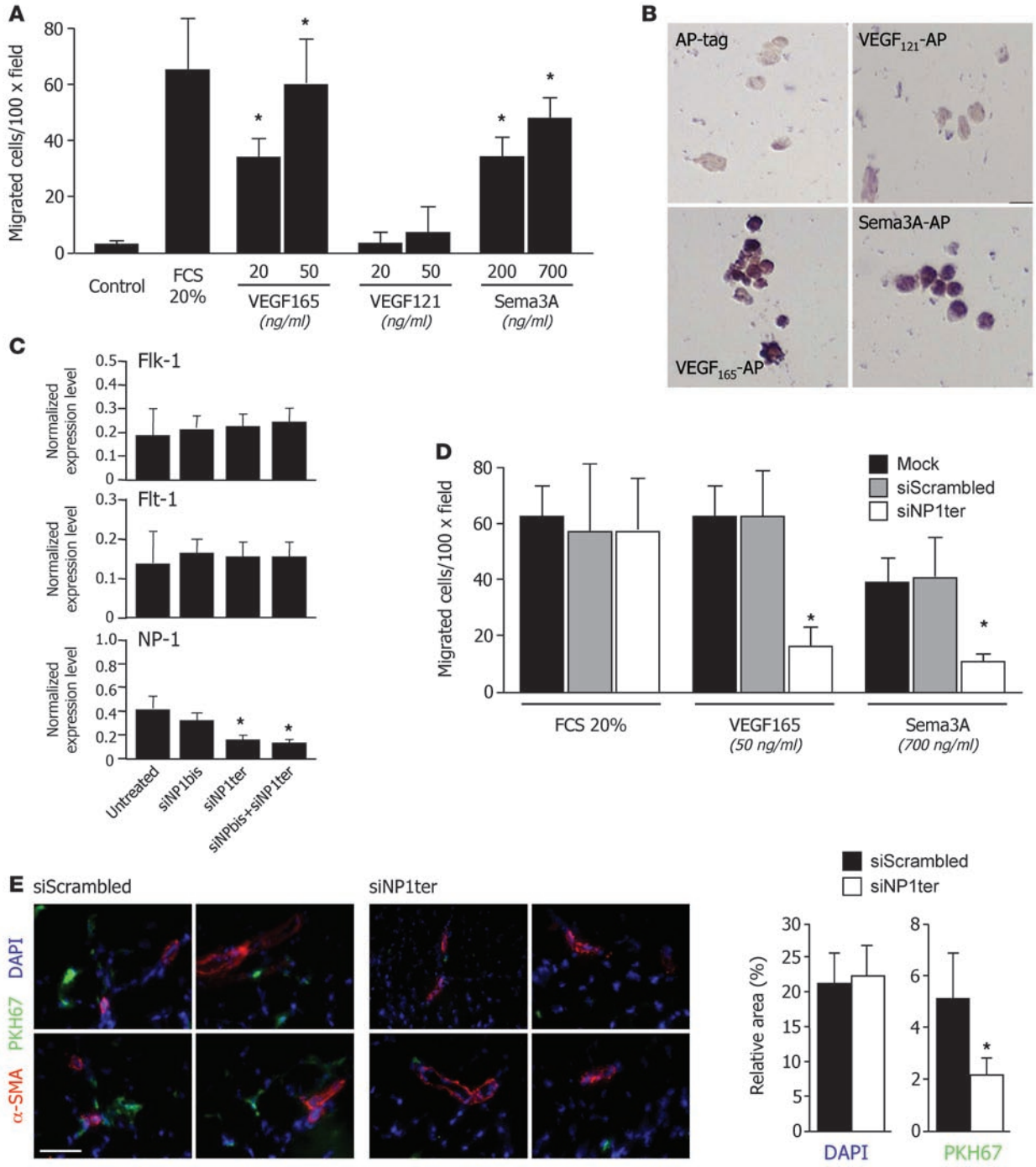

Figure 4

Fundamental role of NP-1 in CD11b$^+$ cell recruitment by $VEGF_{165}$ and Sema3A. (**A**) The number of BM CD11b$^+$ cells migrated in response to different concentrations of $VEGF_{165}$, $VEGF_{121}$, and Sema3A was counted in 8 fields per membrane. Histograms show the mean number of migrated cells ± SD. *$P < 0.05$ over control (no chemoattractant). (**B**) Cell supernatants containing fusion proteins between AP and $VEGF_{165}$, $VEGF_{121}$, or Sema3A were added to CD11b$^+$ cells. Binding was detected upon addition of $VEGF_{165}$-AP and Sema3A-AP, but not $VEGF_{121}$-AP. AP-tag only was used as a negative control. Original magnification, ×20. (**C**) Expression of Flk-1, Flt-1, and NP-1 was analyzed in CD11b$^+$ cells transfected with lipids alone or with siNP1bis and siNP1ter (see Supplemental Figure 4) and normalized to the housekeeping gene *GAPDH*. Shown are means ± SD of 3 independent experiments. *$P < 0.05$ over untreated cells. (**D**) Purified CD11b$^+$ cells were treated with siNP1ter or with a control scrambled siRNA and tested for their ability to migrate in response to $VEGF_{165}$ (50 ng/ml) and Sema3A (700 ng/ml). Silencing of NP-1 (white bars) markedly impaired cell migration to both chemoattractants. Shown are means ± SD of 3 independent experiments. *$P < 0.05$ over untreated cells. (**E**) CD11b$^+$ cells were lipofected with either siNP1ter or the control scrambled siRNA, labeled with the fluorescent dye PKH67, and reinjected i.v. into AAV-$VEGF_{165}$-treated syngeneic mice. Several PKH67-labeled cells (green) were recruited to $VEGF_{165}$-expressing muscles, close to α-SMA–labeled arterioles (red). Conversely, very few siNP1ter-treated cells were found at the site of $VEGF_{165}$-induced angiogenesis, as quantified in the graphs on the right. Shown are means ± SD. $n = 6$. *$P < 0.05$. Scale bar: 50 μm.

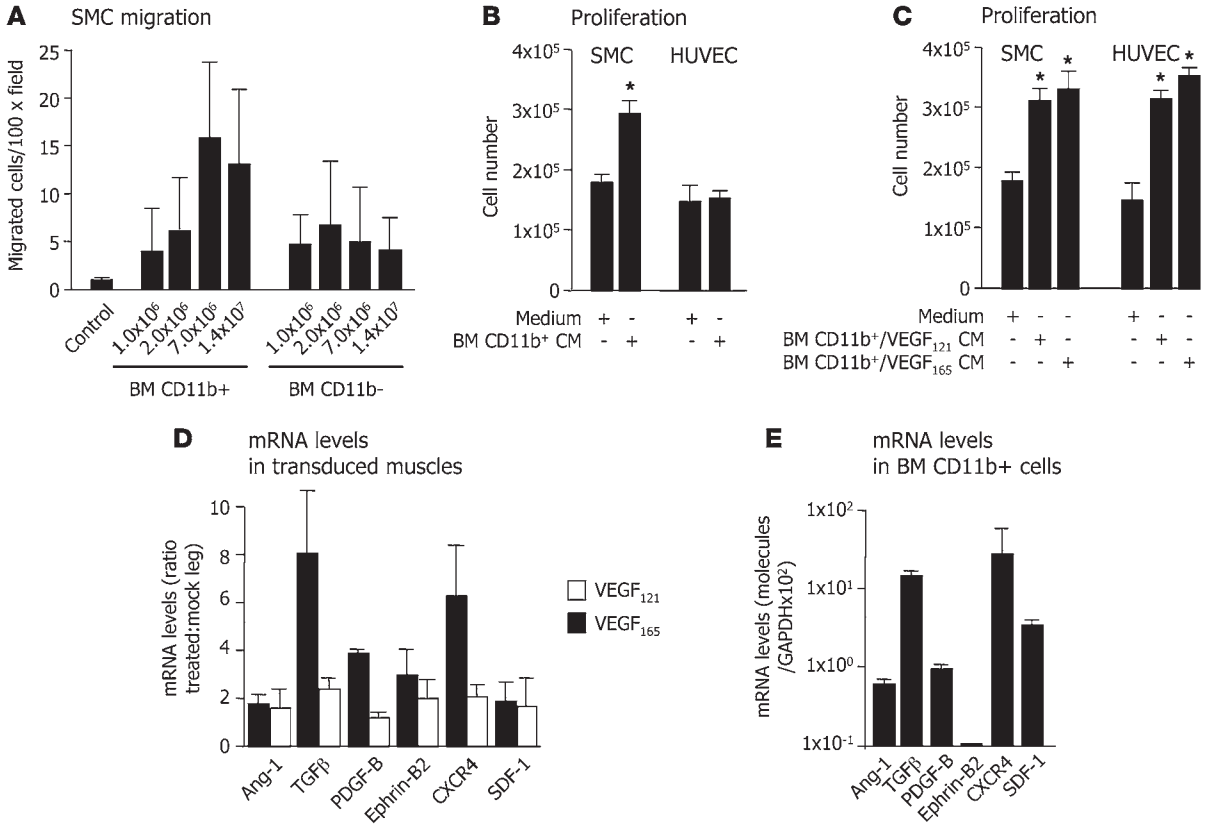

Figure 5

Soluble factors produced by CD11b$^+$ cells stimulate SMC migration and proliferation. (**A**) CD11b$^+$ and CD11b$^-$ cells were used as chemoattractants for primary coronary artery SMCs. Histograms show the mean number of migrated cells ± SD, as counted in more than 8 fields per membrane. Regression analysis indicated that the only supernatant conditioned by CD11b$^+$ cells was able to recruit SMC cells in a dose-related manner ($r = 0.71$; $P < 0.05$). (**B**) SMCs and HUVECS were exposed to medium conditioned by CD11b$^+$ cells, and cell proliferation was measured by MTT assay. SMCs but not HUVECs responded to mitogens secreted by CD11b$^+$ cells. Shown are means ± SD of 3 experiments. *$P < 0.05$ over unstimulated cells; F = 245.0 and 0.32 for SMCs and HUVECs, respectively. (**C**) SMCs and HUVECs were exposed to a medium conditioned by CD11b$^+$ cells previously primed by 50 ng/ml of hrVEGF$_{121}$ or hrVEGF$_{165}$. Upon exposure to both VEGF isoforms, CD11b$^+$ cells became able to stimulate the proliferation of both SMCs (as in **B**) and HUVECs. Shown are means ± SD of 3 experiments. *$P < 0.05$ over unstimulated cells; F = 90.61 and 143.6 for SMCs and HUVECs, respectively. (**D**) The expression levels of a panel of candidate genes were determined by real-time PCR in muscles injected with AAV-VEGF$_{121}$ or AAV-VEGF$_{165}$. Data are presented as a ratio between the VEGF-expressing and the mock-injected contralateral muscles. Shown are means ± SD. $n \geq 6$. (**E**) The same transcripts considered in part **D** were also analyzed in primary CD11b$^+$ BM cells. Shown are means ± SD of 3 independent quantifications.

line phosphatase (AP) bound to cell-surface receptors on CD11b$^+$ cells, consistent with a prominent involvement of the NP-1 receptor in this binding (Figure 4B).

To directly address the role of NP-1 expressed by BM CD11b$^+$ in mediating the recruitment of these cells by VEGF$_{165}$ and Sema3A, we designed 3 siRNAs targeting the NP-1 mRNA (Supplemental Figure 4A). The 2 most active siRNAs (siNP1bis and siNP1ter, which target NP-1 mRNA at positions 2577 and 2860, respectively) were lipofected either alone or in combination into primary CD11b$^+$ cells followed by real-time PCR quantification of Flk-1, Flt-1, and NP-1 transcripts. siNP1ter reduced the levels of overexpressed and endogenous NP-1 by more than 90% and 70%, respectively, in the absence of off-target effects (Figure 4C and Supplemental Figure 4, B–F). siNP1ter-treated CD11b$^+$ cells were then tested for their migratory activity in response to VEGF$_{165}$ or Sema3A. Silencing of NP-1 specifically impaired the migration of CD11b$^+$ cells in response to both chemoattractants, used at their most effective dose. In contrast, the same siRNA had only a modest effect when the same cells were challenged with 20% serum (Figure 4D). This result shows that the chemoattractant activity of VEGF$_{165}$ and Sema3A toward CD11b$^+$ cells is exerted through NP-1. To further confirm the relevance of NP-1 in CD11b$^+$ cell recruitment in vivo, we treated cells with either siNP1ter or a scrambled control siRNA and labeled them with the fluorescent dye PKH67 prior to injection into AAV-VEGF$_{165}$-injected syngeneic animals. As shown in Figure 4E, several control-treated labeled cells were recruited to the site of VEGF$_{165}$ overexpression, whereas very few siNP1ter-treated cells accumulated at these sites.

As NP-1 usually signals through the heterodimerization with other receptors, we sought to determine the involvement of possible NP-1 partners in CD11b$^+$ cell migration. Consistent with the real-time RT-PCR and immunofluorescence results shown in Figure 3, we detected by Western blotting abundant levels of NP-1 and Flt-1 but no expression of NP-2 in primary CD11b$^+$ cells purified from the BM (Supplemental Figure 5A). Flk-1 expres-

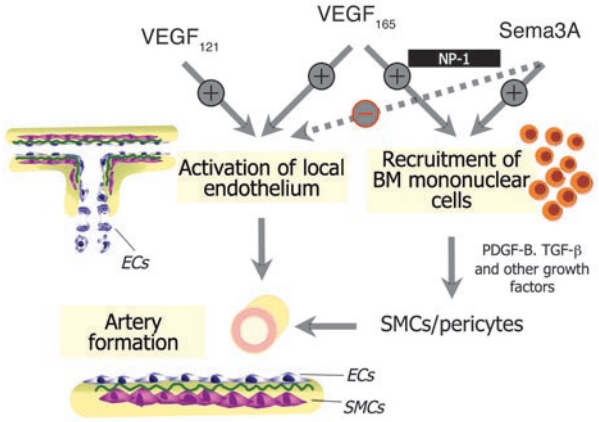

Figure 6
A model to explain the role of BM cells in arteriogenesis. Artery formation relies on the occurrence of 2 concomitant events, namely the activation of the local endothelium (through the canonical VEGF receptors) and the recruitment of BM-derived mononuclear cells through the NP-1 receptor; these cells in turn engage SMCs to the sites of endothelial activation. Only $VEGF_{165}$ is able to stimulate both events and is thus arteriogenic. In contrast, $VEGF_{121}$ activates the endothelium locally, thus inducing capillary sprouting, but is not able to bind NP-1, and thus it does not recruit BM cells nor does it form arteries. Finally, Sema3A, a high-affinity ligand for NP-1, is a potent recruiter of mononuclear cells from the BM, but it exerts an inhibitory effect on endothelial cells and therefore is not angiogenic.

sion could be detected by real-time RT-PCR (Figure 3) but not by Western blotting, likely indicating low levels of expression of this receptor. However, both Flk-1 and Flt-1 coimmunoprecipitated with NP-1, with the signal being even stronger for Flk-1 than for Flt-1. Thus, Flk-1, even if expressed at low levels, is tightly associated to NP-1 in $CD11b^+$ cells (Supplemental Figure 5B). To further validate the presence and activity of the different receptors in $CD11b^+$ cells, we assessed whether their silencing affected cell migration in response to $VEGF_{165}$. As shown in Supplemental Figure 5C, both anti–Flt-1 and anti–Flk-1 siRNAs effectively inhibited cell migration. Interestingly, silencing of plexin-A1, which is also expressed at low levels by $CD11b^+$ cells (not shown), did not have any effect on $CD11b^+$ cell migration.

BM $CD11b^+$ cells stimulate SMC proliferation and migration. The intriguing observation that $VEGF_{121}$ is neither able to bind and recruit BM $CD11b^+$ cells nor to cause the formation of arteries vivo suggests that these cells play an important role during the later phases of the angiogenic process, possibly promoting SMC recruitment and the subsequent formation of arterial vessels. As a first step to verify this hypothesis, we fractionated total BM according to CD11b expression, and both the positive and the negative fractions were tested for their ability to attract primary arterial SMCs. As shown in Figure 5A, the $CD11b^+$ fraction exhibited a marked, dose-dependent chemotactic activity toward SMCs.

Next, we investigated the ability of $CD11b^+$ cells to influence SMC proliferation. We found that the $CD11b^+$ cell–conditioned medium significantly stimulated the proliferation of SMCs; in contrast, no effect could be observed when the same conditioned medium was applied to HUVECs (Figure 5B). This result indicates that unstimulated $CD11b^+$ cells secrete factors able to drive mitogenic signals in SMCs but not in endothelial cells. Of interest, when $CD11b^+$ cells were previously exposed to high doses of $VEGF_{121}$ or $VEGF_{165}$, they acquired the ability to sustain the proliferation of both SMCs and HUVECs to a similar extent (Figure 5C).

Overall, these experiments indicate that BM $CD11b^+$ cells secrete soluble factors able to trigger both the proliferation and the migration of SMCs, thus supporting a possible paracrine action of these cells in the recruitment of SMCs during neovascularization in vivo. To address this issue, we analyzed the expression levels of a panel of molecules previously shown to play a role in vessel maturation. As shown in Figure 5D, muscles injected with AAV-$VEGF_{165}$ exhibited a specific upregulation of TGF-β, PDGF-B, and the CXCR4 chemokine receptor as compared with muscles injected with AAV-$VEGF_{121}$. Interestingly, most of these transcripts were abundantly expressed by primary BM $CD11b^+$ cells (Figure 5E). In contrast, no significant variations could be detected in the expression levels of Ang I, ephrin-B2, and stromal-derived factor-1 (SDF-1) (a CXCR4 ligand). The striking differences detected in the former group of genes cannot be attributed to different levels of expression of $VEGF_{165}$ versus $VEGF_{121}$, as shown by the specific quantification of the human mRNAs expressed from the transduced vectors (Supplemental Figure 2A).

A model to explain the key role of $CD11b^+$ cells in the formation of arterial vessels. Taken together, the results so far described are consistent with a model implying a relevant role of BM $CD11b^+$ cells in promoting the formation of arterial vessels during adult neovascularization (Figure 6). According to this model, both $VEGF_{165}$ and Sema3A share the ability to bind NP-1 and to attract $CD11b^+$ BM cells, which express this receptor. $VEGF_{165}$ and Sema3A, however, have opposite effects on the local endothelium, as the former activates endothelial cell proliferation and migration, while the latter inhibits both processes. In cooperation with the local endothelium activated by $VEGF_{165}$, the recruited myeloid cells in turn promote the maturation of the growing vessels through a paracrine mechanism that determines the enrollment of SMC/pericytes. Thus, arterial formation strictly relies on the simultaneous occurrence of 2 effector mechanisms, namely endothelial cell activation on one side and $CD11b^+$ cell–dependent SMC engagement on the other side.

$CD11b^+$ cells promote vessel maturation and artery formation in vivo. Our model would predict that the combination of $VEGF_{121}$, which activates endothelial cells promoting capillary sprouting, with $CD11b^+$ mononuclear cells, which act in a paracrine fashion by attracting SMCs, should result in the formation of arterial vessels. To validate this prediction in vivo, we injected mice with AAV-$VEGF_{121}$ either alone or in combination with BM $CD11b^+$ cells purified from syngeneic animals. As expected, $VEGF_{121}$ determined massive capillary sprouting, which was evident at both 15 days and 1 month after injection (a representative image is shown in Figure 7A); however, no new arteries were formed. In contrast, in muscles that received the same dose of vector together with 5×10^5 purified $CD11b^+$ cells, a remarkable number of SMC-coated arterial vessels appeared in close proximity to the cellular infiltrates at both 15 days and 1 month after injection (this effect is quantified in Figure 7B, and 3 representative pictures showing artery formation are shown in Figure 7A). No effect at all on either endothelium or arteries was observed by the injection of the cells alone. To confirm the identity of the injected cells and to track their fate in vivo, in a subset of animals, the $CD11b^+$ cells were ex vivo labeled with the lipophilic dye PKH26 immediately prior to injection. When coinjected with AAV-$VEGF_{121}$, these cells were found to persist in the treated

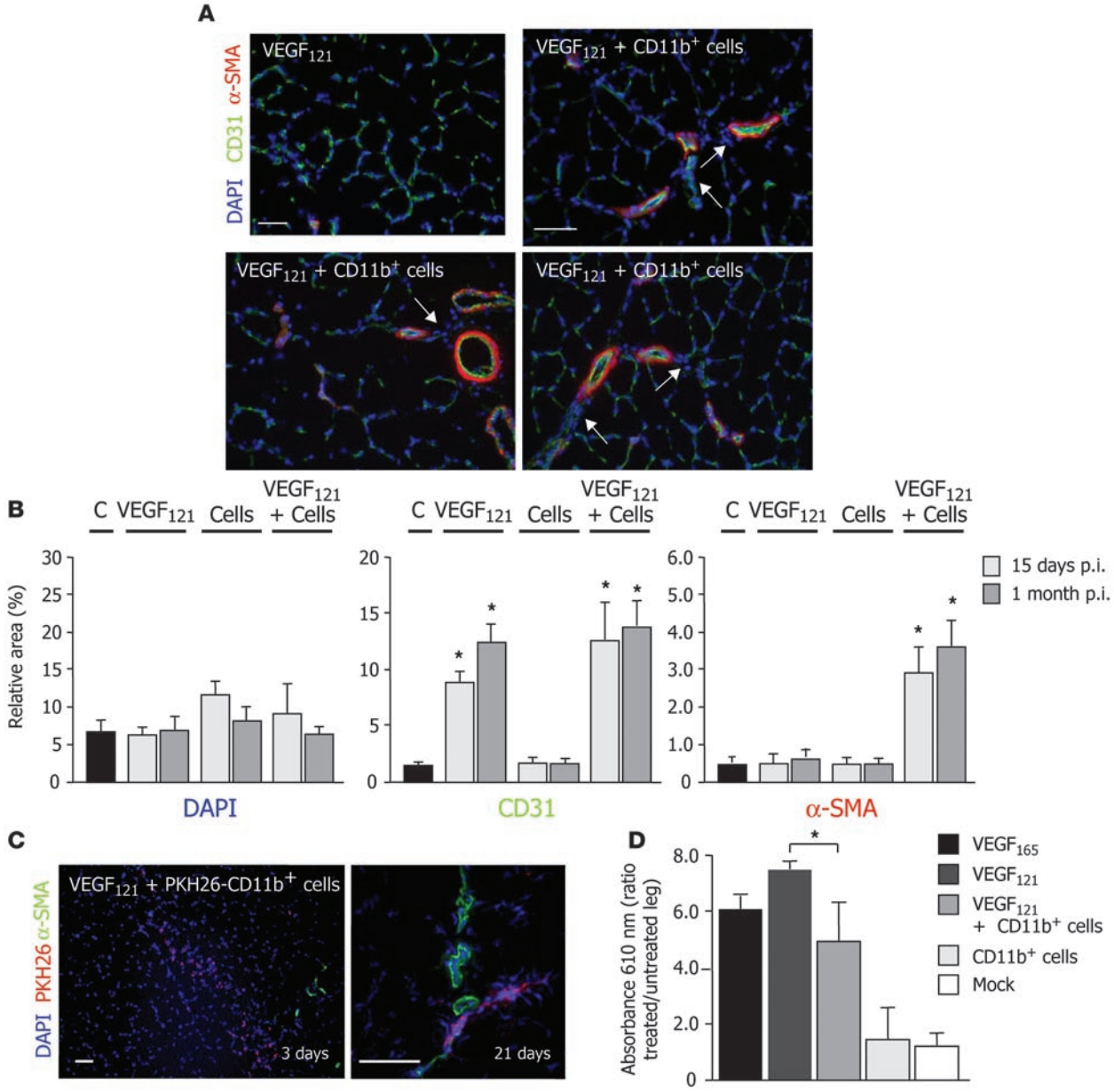

Figure 7

CD11b+ cells promote the formation of arterial vessels through a paracrine effect in concert with the activated endothelium. (**A**) In vivo arterial formation by the coinjection of AAV-VEGF$_{121}$ and CD11b+ cells. While AAV-VEGF$_{121}$ only promotes massive capillary sprouting, as shown by CD31 staining in green (upper left panel), the simultaneous administration of purified CD11b+ cells determines the formation of several arteries (α-SMA staining in red) in close proximity to the cellular infiltrates (white arrows). Scale bar: 100 μm. (**B**) Quantification of the relative areas occupied by cellular nuclei (DAPI), endothelial cells (CD31), or SMCs (α-SMA) in 20 independent sections for each treatment (AAV-VEGF$_{121}$, BM CD11b+ cells, or a combination of both). Data are presented as means ± SD. *Statistical significance over control, AAV-LacZ–treated muscles ($P < 0.05$). Cells, BM CD11b+ cells; C, control. (**C**) CD11b+ cell engraftment in the skeletal muscle. A large number of PKH26-labeled CD11b+ cells injected together with AAV-VEGF$_{121}$, could be detected in the skeletal muscle as red fluorescent cells at day 3 after injection (left panel). A lower number of cells were still present at longer time points (shown at 21 days on the right panel) in close proximity to arterial vessels (visualized in green by α-SMA immunofluorescence staining). Scale bar: 200 μm. (**D**) Effect of CD11b+ cells on VEGF$_{121}$-induced vascular leakiness. Shown are results of the Miles test as a measure of vascular permeability in muscles injected with AAV- VEGF$_{165}$ and VEGF$_{121}$ alone or in combination with CD11b+ cells. Data are presented as a ratio of the adsorbance for the treated and the contralateral mock-treated tibialis anterior muscle. A significant reduction in vascular leakiness was evident when CD11b+ cells had been coinjected with AAV-VEGF$_{121}$ as compared with AAV-VEGF$_{121}$ alone, reaching a value comparable to AAV-VEGF$_{165}$. No effect was observed by CD11b+ cell injection per se. *$P < 0.05$.

muscles for at least 3 weeks after transplantation (Figure 7C). Of interest, the simultaneous staining of arterial vessels using an anti–α-SMA antibody revealed that several of these cells were positioned in close proximity to the arterial vessel wall.

Since the acquisition of an SMC layer has been traditionally considered a fundamental maturation step during the angiogenic process, we investigated to determine whether the arteriogenic effect driven by the simultaneous injection of AAV-$VEGF_{121}$ with purified $CD11b^+$ cells also determined a functional improvement of the newly formed vasculature. To this aim, we compared the vascular leakiness of muscles treated with AAV- $VEGF_{165}$, AAV-$VEGF_{121}$ alone, or AAV-$VEGF_{121}$ in combination with $CD11b^+$ cells by a modification of the Miles test, performed by systemically injecting a bolus of Evans blue dye (23). As shown in Figure 7D, both $VEGF_{165}$ and $VEGF_{121}$ determined the formation of leaky vessels, with extravasation of the dye being higher in the $VEGF_{121}$-treated muscles. Conversely, the simultaneous injection of $CD11b^+$ cells together with AAV-$VEGF_{121}$ significantly counteracted the permeabilizing effect of this factor. This result clearly indicates that, besides morphological evidence of arterial formation, $CD11b^+$ cells also exert a promaturation activity on the newly formed vasculature.

Discussion

Here, we propose a new model for the generation of arterial vessels in adult organisms, according to which NP-1–expressing $CD11b^+$ cells attracted from the BM to the site of neoangiogenesis are essential for the recruitment and proliferation of SMCs around the growing capillaries, which leads to the formation of new arteries. This conclusion is based on the following experimental observations: (a) arterial formation in nonischemic, adult tissues is accompanied by the infiltration of BM-derived mononuclear cells; (b) formation of new arteries is specifically induced by $VEGF_{165}$; $VEGF_{121}$ neither is arteriogenic nor does it recruit BM cells; (c) $VEGF_{165}$, but not $VEGF_{121}$, binds the NP-1 receptor; (d) both BM $CD11b^+$ cells and the mononuclear cells infiltrating the sites of artery formation express abundant levels of NP-1; silencing of this receptor by RNAi impairs the migratory capacity of $CD11b^+$ cells in response to both $VEGF_{165}$ and Sema3A both in vitro and in vivo; and (e) BM $CD11b^+$ cells activate SMC proliferation and migration in vitro and promote the formation of new SMC-coated arteries in vivo.

The observation that $VEGF_{121}$ is capable neither of recruiting BM cells nor of forming arteries in vivo points to an essential role of these cells in the specific process of arterial formation. This conclusion is in perfect agreement with the notion that knockout mice expressing only $VEGF_{120}$ exhibit specific defects in arterial development (3–5). In this respect, it is worth mentioning that the difference in arteriogenic potential between $VEGF_{121}$ and $VEGF_{165}$ has probably escaped previous gene transfer investigations, since the vast majority of studies were performed by exploiting first generation adenoviral vectors (29–31) or ex vivo–engineered myoblasts (24, 32). The former system is highly inflammatory and induces a strong immunogenic response, while the latter leads to VEGF production at such high levels that aberrant vascular structures appear in treated tissues. In both cases, vector or cell injection per se induces the recruitment of inflammatory cells (including myeloid cells) that might contribute to arterial formation. Similar considerations also apply to studies performed in ischemic models, in which the massive infiltration of inflammatory cells determined by acute ischemia blurs the differential capacity of the 2 VEGF isoforms to recruit myeloid cells. Appreciation of the fact that $VEGF_{121}$ has different angiogenic properties compared with $VEGF_{165}$ is relevant for the choice of the appropriate gene in the gene therapy trials aiming at therapeutic angiogenesis, since the formation of larger arterial vessels in addition to capillaries is an essential requisite to obtaining functional neovascularization.

Besides the property of binding to heparin, the main difference that distinguishes $VEGF_{165}$ and $VEGF_{121}$ is the ability of the former factor to interact with NP-1, at least at the physiological concentrations and in vivo conditions used in our study. Indeed, we found that NP-1 was highly expressed by purified BM $CD11b^+$ cells as well as by the cells infiltrating the sites of neoangiogenesis. In addition, this receptor was essential to mediating the chemoattractive activity of both $VEGF_{165}$ and Sema3A on $CD11b^+$ cells in vitro and in vivo. Collectively, these results indicate that NP-1 exerts a prominent and essential role mediating in the recruitment of $CD11b^+$ cells. We also observed that these cells expressed, albeit at lower levels, both Flt-1 and Flk-1 and that the downregulation of these receptors impaired $CD11b^+$ migration in response to $VEGF_{165}$ and Sema3A. It might thus be conceivable that Flt-1 and Flk-1 act as NP-1 coreceptors in this process. Of note, however, VEGF121 was neither able to bind $CD11b^+$ cells (in contrast with previous findings in which the factor was used at very high concentrations; ref. 33) nor to determine their migration, thus indicating that the engagement of NP-1 is necessary for both events.

Despite acting as a powerful $CD11b^+$ cell attractor, Sema3A potently inhibited VEGF-induced angiogenesis. To our knowledge, this is the first demonstration that Sema3A, in addition to its inhibitory role on blood vessel formation during development (34, 35), also exerts an antiangiogenic activity in adult organisms. The exact mechanism of this inhibition still remains to be elucidated. Indeed, this event might simply depend on a competition between $VEGF_{165}$ and Sema3A for binding to Flk-1 on endothelial cells (6) or it might reflect a specific signaling activity of Sema3A on growing vessels. Our findings that Sema3A also inhibits $VEGF_{121}$-induced angiogenesis and that apoptotic endothelial cells are detected in muscles coinjected with AAV-$VEGF_{165}$ and AAV-Sema3A are consistent with the conclusion that Sema3A exerts a proapoptotic activity on VEGF-activated endothelial cells. Whether this activity is direct and VEGF specific or somehow involves the recruited cells and extends to other angiogenic inducers still remains unexplored.

A number of studies are concordant in concluding that cells deriving from the BM are an essential component of both normal and tumor angiogenesis, although controversy still exists about the possibility that they might themselves become part of the vessels. The BM-derived cells that infiltrate the muscles expressing $VEGF_{165}$ in our experimental conditions are definitely not incorporated into the newly formed vasculature to become $CD31^+$ endothelial cells or $\alpha\text{-SMA}^+$ SMCs (25). This is in agreement with several investigations that have exploited other angiogenesis models (14, 22, 24, 36, 37). Obviously, we cannot exclude that in other conditions, such as during tumor angiogenesis, a subset of BM-derived cells might act as pericyte progenitors that are directly incorporated into the vasculature (38). Whether this subset of cells might also be recruited using the NP-1 receptor might become the subject of future investigation.

Collectively, our data lead to the conclusion that artery formation relies on 2 essential components: on one side, stimulation of the local endothelium (most likely through the canonical VEGF receptors), while on the other side, recruitment of circulating myeloid cells through the NP-1 receptor. Striking evidence that recapitulates this notion comes from 2 main findings: (a) the reduced homing capacity of myeloid cells in which NP-1 has been silenced; and (b) the appearance of arterial vessels upon the direct injection of BM CD11b$^+$ cells together with the AAV vector expressing $VEGF_{121}$. The latter finding rules out the possibility that the different angiogenic effects exerted by $VEGF_{165}$ and $VEGF_{121}$ might only depend on their diverse ability to interact with NP-1 on the arterial endothelium and points to a major role of the recruited cells in determining the formation of novel arteries.

Our observations indicate that BM cells act in a paracrine fashion by specifically promoting vessel maturation to form arterioles. Consistent with this conclusion, studies on embryonic vascular development have revealed that cells of the vessel wall are added at later stages of vessel assembly through the differentiation of mural precursors upon stimulation by soluble factors (39). According to previous gene knockout studies, plausible candidates that are likely to play a major role in this process essentially belong to the Ang I/Tie2, TGF-β/TGFR-β, and PDGF-B/PDGFR-β systems (39–42). In particular, the hearts of *VEGF$^{120/120}$* mice, showing impaired arterial formation, expressed reduced levels of PDGF-B and its type β receptor, whereas the levels of Ang I were similar (3). Accordingly, we also observed increased expression of TGF-β and PDGF-B in the muscles overexpressing $VEGF_{165}$ and no significant differences in the levels of Ang I.

Recent work has indicated that SDF-1 is essential to retaining CD45$^+$CD11b$^+$ myeloid cells to the sites of neoangiogenesis and to promoting their correct positioning on the external side of the vessel wall (22). In keeping with these results, we found that CXCR4 (the main receptor for SDF-1) was significantly upregulated in the $VEGF_{165}$-expressing tissues. However, no upregulation was detected for SDF-1, which was already constitutively expressed at high levels in untreated muscles.

A final issue that still remains to be understood is to what extent the process of new artery formation, which we describe as dependent on both local endothelial cell activation and BM-derived cell recruitment, overlaps with the traditional concept of "arteriogenesis," as referring to the remodeling of preexisting vessels to form larger collateral conductance arteries (43). In this context, it is worth mentioning that, although arteriogenesis is mainly triggered by increased shear stress, different experimental models suggest that this process is always accompanied by tissue infiltration by monocytes and macrophages (18, 43–45), suggesting that these cells might also play a role in the formation of larger conductance arteries. In this respect, our results might also explain the benefits conferred by the injection of autologous BM cells in patients with myocardial or peripheral ischemia even in the absence of clear proof of transdifferentiation of the transplanted cells (46–50).

Methods

Recombinant AAV vectors and animal treatment. The rAAV vectors used in this study were produced by the AAV Vector Unit at ICGEB Trieste (http://www.icgeb.org/RESEARCH/TS/COREFACILITIES/AVU.htm), according to the protocol previously described (23). All the vectors used in this study express the various human cDNAs under investigation ($VEGF_{165}$, $VEGF_{121}$, Sema3A) or the *LacZ* gene under the control of the constitutive CMV immediate early promoter. All the viral stocks used in this study had a titer greater than or equal to 1×10^{12} viral genome particles/ml. The proper expression of all transgenes was tested in vitro by Western blotting using specific antibodies after transduction of 293T cells and in vivo by real-time PCR quantification of the transgene mRNAs in transduced tissues.

Mice were injected in the tibialis anterior with 50 μl of each vector. Animal care and treatment were conducted in conformity with institutional guidelines in compliance with national and international laws and policies (EEC Council Directive 86/ 609, OJ L 358. December 12, 1987). All animal studies were approved by the Italian Ministry of Health, Office X, according to DL 116/92 of the Republic of Italy and by the ICGEB Management Board, Trieste, Italy.

Primary cell cultures. CD11b$^+$ cells were isolated from total BM (extracted from tibiae and femurs of BALB/c mice) using CD11b magnetic cell separation system beads (Miltenyi Biotec) and cultured in RPMI 1640 supplemented with 10% high-quality FBS (GIBCO). In a subset of experiments of in vivo cell transplantation, CD11b$^+$ cells were labeled with PKH26 red fluorescent linker (Sigma-Aldrich) immediately after purification and prior to injection. Coronary artery SMCs and HUVECs were purchased from Clonetics (Clonetics; Cambrex) and cultured in their own media, provided by the manufacturer.

Real-time PCR. Total RNA from purified CD11b$^+$ cells or microdissected tissue samples was extracted using TRIzol reagent (Invitrogen) according to manufacturer instructions and reverse transcribed using hexameric random primers. The cDNA was then used as a template for real-time PCR amplification to detect the expression levels of the murine VEGF and Sema3A receptors (VEGFR-1, VEGFR-2, NP-1, and NP-2), as well as of TGF-β, PDGF-B, CXCR4, angiopoietin-1, ephrin-B2, and SDF-1; the housekeeping genes *GAPDH* and *18S* were used to normalize the results. All the amplifications were performed on an ABI PRISM 7000 Instrument (Applied Biosystems) using predeveloped assays (Applied Biosystems).

BM and cell transplantation studies. BM transplantation studies were performed as already described (25). Recipient, age-matched syngeneic female mice were lethally irradiated with a total dose of 8.5 Gy; 2×10^6 cells BM cells, obtained from male mice, resuspended in 0.2 ml medium, were transplanted via tail-vein injection. After 4 weeks, blood counts and hematocrit values confirmed the full hematopoietic recovery.

Successful engraftment of the transplanted cells was further confirmed by the quantification of a specific mouse Y chromosome sequence in DNA samples extracted from PBMC or BM cells at 1, 2, and 6 months after transplantation, using primers Y-F (5′-CATGCAAAATACAGAGATCA-3′) and Y-R (5′-TAAAATGCCACTCCTCTGTG-3′) to produce a genomic segment of 181 bp.

As a cellular reference gene, mouse β-globin was amplified by primers BG-F (5′-CAGCCTCAAGGGCACCTTTG-3′) and BG-R (5′-AGCAGCAATTCTGAATAGAG-3′) to generate a 238-bp fragment. Exact quantification was obtained using an established competitive PCR procedure that uses a synthetic DNA competitor for the quantification of both targets (51).

To monitor the recruitment of CD11b$^+$ cells in vivo, 5×10^6 cells purified by the use of magnetic beads were lipofected with either siNP1ter or a control scrambled siRNA, labeled with green dye PKH67 (Sigma-Aldrich), and injected i.v. into syngeneic mice, previously transduced i.m. with AAV-$VEGF_{165}$.

In vivo perfusion with fluorescent microspheres. To quantify the vascular volume of treated and untreated muscles, 300 μl of orange fluorescent microspheres (FluoSpheres; Molecular Probes) were injected i.v. into living mice. After 1 minute (to ensure a proper distribution of the microspheres throughout the body), animals were sacrificed and both tibialis

anterior muscles immediately harvested. Recovery of microspheres and extraction of fluorescent dye was performed according to manufacturers' instructions. In brief, weighted muscles were digested in 2 M ethanolic KOH, 0.5% Tween-80 (v/v) (Sigma-Aldrich) at 60°C with periodic shaking. Homogenates were centrifuged in a swinging rotor and the pellet resuspended in 0.25% Tween-80. After an additional centrifugation and washing, microspheres were dissolved in 2-ethoxyethyl acetate (Sigma-Aldrich). Debris was removed by centrifugation, and fluorescence in the supernatant was measured with the VersaFluor Fluorometer System (Bio-Rad). Values were normalized and expressed as ratios between fluorescence of treated and untreated contralateral muscle for each animal (n = 6 per group).

To obtain a 3D reconstruction of the vascular network, mice were subjected to in vivo perfusion with a 1:6 dilution of the same fluorescent microsphere solution (FluoSpheres; Molecular Probes). After anesthesia, the chest was opened and the vasculature perfused with PBS for 3 minutes, followed by 20 ml of FluoSpheres (1:6 dilution of the stock) via a blunt 13-gauge needle inserted through the left ventricle into the ascending aorta. The treated muscles were removed and immediately frozen for cryosectioning. Thick (50–100 μm) sections were analyzed by confocal microscopy to obtain a Z-stack for the 3D reconstruction of the vascular network.

Migration assay. Migration assays were performed with the use of 5-μm (for $CD11b^+$ cells) or 8-μm (for SMCs and endothelial cells) pore size transwell permeable supports with a polycarbonate membrane (Costar; Corning Inc.). 1×10^5 cells were seeded in serum-free medium in the upper chamber, while chemoattractants were placed in the lower chamber. After 16 hours incubation, migrated cells on the lower surface of the membrane were fixed in methanol and stained with Giemsa. Each assay was carried out in triplicate, by counting 8 fields per membrane at ×400 magnification. Results are expressed as the mean number of migrated cells ± SD. $hrVEGF_{121}$, $VEGF_{165}$, and hrSema3A were purchase from R&D.

MTT proliferation assay. HUVEC and SMC proliferation were estimated by the 3-(4,5-dimethylthiazol-2-yl)-2,5-diphenyltetrazolium bromide (MMT) colorimetric assay. Purified $CD11b^+$ cells were treated with 50 ng/ml of $hrVEGF_{121}$ or $VEGF_{165}$ every 12 hours for 72 hours. At regular intervals, condition medium was added to HUVECs or SMCs plated in a 96-multiwell plate. At the end of the incubation time, culture medium was removed and 100 μl of MTT (5 mg/ml) (Roche Molecular Biochemicals) was added to each well for 4 hours. The precipitated MTT formazan was dissolved in a mixture of 100 μl of 10% and 10 μM HCl, and the absorbance read the day after at 570 nm with an ELISA Reader (Bio-Rad). Cell number was determined from absorbance values by using a preestablished calibration curve.

Vessel wall permeability assay. Analysis of vessel permeability was performed by an adaptation of the Miles assay (52) to rodent muscles. Mice (n = 6 per group) were injected in the jugular vein with 250 μl of 0.5% Evans blue (Sigma-Aldrich), respectively, and sacrificed after 30 minutes. The tibialis anterior muscles were removed and weighed. The dye was extracted by incubation in 2% formamide at 55°C and quantified spectrophotometrically at 610 nm. Absorbance values were converted according to a standard curve in Evans blue concentration and expressed as a ratio between treated and control muscles from the same animal.

Histology. For histological evaluation, tissue samples were either snap frozen or fixed in 2% formaldehyde and embedded in paraffin. Immunohistochemistry was performed on paraffin-embedded sections, with the use of the following antibodies: mouse monoclonal against α-SMA (clone 1A4, Sigma-Aldrich) and rabbit polyclonal against cleaved caspase-3 (Cell Signaling). Protocols were according to the Vectastain Elite ABC kit (universal or goat) from Vector Laboratories. After treatment, slides were rinsed in PBS and signals were developed using 3,3′-diaminobenzidine as a substrate for the peroxidase chromogenic reaction (Lab Vision Corp.).

For immunofluorescence, frozen sections (5 μm thick) were fixed in cold acetone and blocked for 30 minutes with 5% goat or 5% horse serum in PBS, depending on the secondary antibody. The following primary antibodies were used diluted 1:200 in blocking buffer: anti-CD11b, anti-CD31, anti-CD45 (all from BD Biosciences — Pharmingen), anti–NP-1 and anti–NP-2 (both from R&D Systems), and Cy3-conjugated anti–α-SMA (clone 1A4) (Sigma-Aldrich). Relative areas occupied by differently stained cells were quantified by the use of ImageJ software.

For the staining of whole-animal vasculature with fluoresceinated lectin, 100 μl of *Lycopersicum esculentum* lectin (Vector Laboratories) was injected into living mice through the jugular vein to ensure its systemic distribution. After 15 minutes, mice were anesthetized and in vivo perfused with 1% paraformaldehyde via a blunt 13-gauge needle inserted through the left ventricle into the ascending aorta. The treated muscles were removed and immediately frozen for cryosectioning. 100-μm–thick sections were analyzed by confocal microscopy to obtain a Z-stack for the 3D reconstruction of the vascular network.

Laser microdissection. For microdissection, cryosections (10 μm) from muscles treated either with AAV-$VEGF_{165}$ or AAV-Sema3A were mounted on glass slides. After hematoxylin staining for 45 seconds, the sections were subsequently immersed in 70% and 96% ethanol and stored in 100% ethanol until use. No more than 10 sections were prepared at once to reduce the storage time. Cellular infiltrates having a diameter of 100–500 μm were selected and microdissected under optical control using the Laser Microbeam System (PALM Microlaser Technologies GmbH). Afterwards, tissue particles were collected in TRIZOL (Invitrogen) for RNA extraction, according to the manufacturer's instructions.

Synthesis and validation of NP-1–specific siRNAs. siRNAs targeting NP-1 mRNA were designed according to the rules suggested by Elbashir et al. (53) and synthesized as shRNAs using the AmpliScribe T7 High Yield Transcription Kit (Epicenter Technologies) according to manufacturer's instructions.

siRNA efficiency was validated by cotransfecting each shRNA together with the chimeric plasmid pEGFP–NP-1 in HEK293T human embryonic kidney cell line, as schematically represented in Supplemental Figure 4B. The number of EGFP-positive cells was determined 36 hours after transfection by cytofluorimetric analysis (FACScalibur; BD). A control, scrambled siRNA for siNP1ter was also generated by using the siRNA Wizard tool (http://www.sirnawizard.com).

Site-directed mutagenesis. Site-directed mutagenesis was performed on NP-1 cDNA by using the QuickChange Site-Directed Mutagenesis Kit (Stratagene). In brief, primers containing the desired point mutations were designed and pEGFP–NP-1 was used as template for PCR amplification. PCR amplicons were digested with DpnI to erase the methylated, nonmutated parental DNA.

AP ligand–binding assay. $CD11b^+$ cells from BALB/c mice were seeded on poly-lysine–coated slides, fixed with 70% ethanol, and incubated overnight with supernatants from HEK293 cells overexpressing $VEGF_{165}$-AP, $VEGF_{121}$-AP, Sema3A-AP, and AP-tag, the last as a negative control. After additional fixation in 60% acetone, 4% PFA, and 40 mM HEPES, pH 7.0, a coloring reaction was developed by using NBT/BCIP tablets (Roche).

Coimmunoprecipitation and Western blotting. Immunoprecipitation was performed starting with 2×10^8 $CD11b^+$ cells from BALB/c mice stimulated with 50 ng/ml $rhVEGF_{165}$ (30 minutes on ice, followed by 7 minutes at 37°C) and lysed in a buffer containing 150 mM NaCl, 20 mM Tris, pH 7.5, 1% Triton X-100, protease inhibitor (tablets; Roche) and phosphatase inhibitors (10 mM NaF, 1 mM Na_3VO_4). For each point, 1.4 mg total proteins were immunoprecipitated using anti–NP-1

(sc-7239; Santa Cruz Biotechnology Inc.), anti–Flt-1 (sc-316; Santa Cruz Biotechnology Inc.), and anti–Flk-1 antibodies (sc-504-AC; Santa Cruz Biotechnology Inc.).

Proteins were resolved by 8% SDS-PAGE and visualized with anti–NP-1 (c-19; Santa Cruz Biotechnology Inc.), anti-NP2 (AF567, R&D), anti–Flk-1 (sc-504; Santa Cruz Biotechnology Inc.), anti–Flt-1 (c-17; Santa Cruz Biotechnology Inc.), and anti-Hsp70 (SPA-815; StressGen) antibodies.

Statistics. One-way ANOVA and Bonferroni-Dunn post hoc test were used to compare multiple groups. Pairwise comparison between groups was performed using the Student's *t* test. Dose-response effect was assessed by regression analysis. $P < 0.05$ was considered statistically significant.

Acknowledgments

The authors are grateful to Marina Dapas, Sara Tomasi, and Michela Zotti for their outstanding technical support and to Mauro Sturnega for his invaluable help in animal experimentation. We also thank Suzanne Kerbavcic for precious editorial assistance. This work was supported by grants from the FIRB program of the "Ministero dell'Istruzione, Universita' e Ricerca," Italy and from the "Fondazione CR Trieste" of Trieste, Italy.

Received for publication May 29, 2007, and accepted in revised form April 9, 2008.

Address correspondence to: Mauro Giacca, ICGEB Trieste, Padriciano 99, 34012 Trieste, Italy. Phone: 39-040-375-7324; Fax: 39-040-375-7380; E-mail: giacca@icgeb.org.

Mauro Giacca is on leave of absence from the Department of Biomedicine, Faculty of Medicine, University of Trieste, Trieste, Italy.

1. Ferrara, N., Gerber, H.P., and LeCouter, J. 2003. The biology of VEGF and its receptors. *Nat. Med.* **9**:669–676.
2. Carmeliet, P. 2005. Angiogenesis in life, disease and medicine. *Nature.* **438**:932–936.
3. Carmeliet, P., et al. 1999. Impaired myocardial angiogenesis and ischemic cardiomyopathy in mice lacking the vascular endothelial growth factor isoforms VEGF164 and VEGF188. *Nat. Med.* **5**:495–502.
4. Mattot, V., et al. 2002. Loss of the VEGF(164) and VEGF(188) isoforms impairs postnatal glomerular angiogenesis and renal arteriogenesis in mice. *J. Am. Soc. Nephrol.* **13**:1548–1560.
5. Stalmans, I., et al. 2002. Arteriolar and venular patterning in retinas of mice selectively expressing VEGF isoforms. *J. Clin. Invest.* **109**:327–336.
6. Miao, H.Q., et al. 1999. Neuropilin-1 mediates collapsin-1/semaphorin III inhibition of endothelial cell motility: functional competition of collapsin-1 and vascular endothelial growth factor-165. *J. Cell Biol.* **146**:233–242.
7. Jia, H., et al. 2006. Characterization of a bicyclic peptide neuropilin-1 (NP-1) antagonist (EG3287) reveals importance of vascular endothelial growth factor exon 8 for NP-1 binding and role of NP-1 in KDR Signaling. *J. Biol. Chem.* **281**:13493–13502.
8. Soker, S., Takashima, S., Miao, H.Q., Neufeld, G., and Klagsbrun, M. 1998. Neuropilin-1 is expressed by endothelial and tumor cells as an isoform- specific receptor for vascular endothelial growth factor. *Cell.* **92**:735–745.
9. Kolodkin, A.L., et al. 1997. Neuropilin is a semaphorin III receptor. *Cell.* **90**:753–762.
10. Kawasaki, T., et al. 1999. A requirement for neuropilin-1 in embryonic vessel formation. *Development.* **126**:4895–4902.
11. Kitsukawa, T., Shimono, A., Kawakami, A., Kondoh, H., and Fujisawa, H. 1995. Overexpression of a membrane protein, neuropilin, in chimeric mice causes anomalies in the cardiovascular system, nervous system and limbs. *Development.* **121**:4309–4318.
12. Rafii, S. 2000. Circulating endothelial precursors: mystery, reality, and promise. *J. Clin. Invest.* **105**:17–19.
13. Urbich, C., and Dimmeler, S. 2004. Endothelial progenitor cells: characterization and role in vascular biology. *Circ. Res.* **95**:343–353.
14. Ziegelhoeffer, T., et al. 2004. Bone marrow-derived cells do not incorporate into the adult growing vasculature. *Circ. Res.* **94**:230–238.
15. Wagers, A.J., Sherwood, R.I., Christensen, J.L., and Weissman, I.L. 2002. Little evidence for developmental plasticity of adult hematopoietic stem cells. *Science.* **297**:2256–2259.
16. Rosenzweig, A. 2006. Cardiac cell therapy--mixed results from mixed cells. *N. Engl. J. Med.* **355**:1274–1277.
17. Heil, M., et al. 2004. Collateral artery growth (arteriogenesis) after experimental arterial occlusion is impaired in mice lacking CC-chemokine receptor-2. *Circ. Res.* **94**:671–677.
18. Arras, M., et al. 1998. Monocyte activation in angiogenesis and collateral growth in the rabbit hindlimb. *J. Clin. Invest.* **101**:40–50.
19. Imada, T., et al. 2005. Targeted delivery of bone marrow mononuclear cells by ultrasound destruction of microbubbles induces both angiogenesis and arteriogenesis response. *Arterioscler. Thromb. Vasc. Biol.* **25**:2128–2134.
20. Hoefer, I.E., et al. 2005. Leukocyte subpopulations and arteriogenesis: specific role of monocytes, lymphocytes and granulocytes. *Atherosclerosis.* **181**:285–293.
21. Dor, Y., et al. 2002. Conditional switching of VEGF provides new insights into adult neovascularization and pro-angiogenic therapy. *EMBO J.* **21**:1939–1947.
22. Grunewald, M., et al. 2006. VEGF-induced adult neovascularization: recruitment, retention, and role of accessory cells. *Cell.* **124**:175–189.
23. Arsic, N., et al. 2003. Induction of functional neovascularization by combined VEGF and angiopoietin-1 gene transfer using AAV vectors. *Mol. Ther.* **7**:450–459.
24. Springer, M.L., et al. 2003. Localized arteriole formation directly adjacent to the site of VEGF-induced angiogenesis in muscle. *Mol. Ther.* **7**:441–449.
25. Zentilin, L., et al. 2006. Bone marrow mononuclear cells are recruited to the sites of VEGF-induced neovascularization but are not incorporated into the newly formed vessels. *Blood.* **107**:3546–3554.
26. Zacchigna, S., et al. 2005. Improved survival of ischemic cutaneous and musculocutaneous flaps after vascular endothelial growth factor gene transfer using adeno-associated virus vectors. *Am. J. Pathol.* **167**:981–991.
27. Ferrarini, M., et al. 2006. Adeno-associated virus–mediated transduction of VEGF165 improves cardiac tissue viability and functional recovery after permanent coronary occlusion in conscious dogs. *Circ. Res.* **98**:954–961.
28. Neufeld, G., Cohen, T., Gengrinovitch, S., and Poltorak, Z. 1999. Vascular endothelial growth factor (VEGF) and its receptors. *FASEB J.* **13**:9–22.
29. Gowdak, L.H., et al. 2000. Adenovirus-mediated VEGF(121) gene transfer stimulates angiogenesis in normoperfused skeletal muscle and preserves tissue perfusion after induction of ischemia. *Circulation.* **102**:565–571.
30. Rajagopalan, S., Shah, M., Luciano, A., Crystal, R., and Nabel, E.G. 2001. Adenovirus-mediated gene transfer of VEGF(121) improves lower-extremity endothelial function and flow reserve. *Circulation.* **104**:753–755.
31. Rosengart, T.K., et al. 1999. Angiogenesis gene therapy: phase I assessment of direct intramyocardial administration of an adenovirus vector expressing VEGF121 cDNA to individuals with clinically significant severe coronary artery disease. *Circulation.* **100**:468–474.
32. Springer, M.L., Chen, A.S., Kraft, P.E., Bednarski, M., and Blau, H.M. 1998. VEGF gene delivery to muscle: potential role for vasculogenesis in adults. *Mol. Cell.* **2**:549–558.
33. Pan, Q., et al. 2007. Neuropilin-1 binds to VEGF121 and regulates endothelial cell migration and sprouting. *J. Biol. Chem.* **282**:24049–24056.
34. Serini, G., et al. 2003. Class 3 semaphorins control vascular morphogenesis by inhibiting integrin function. *Nature.* **424**:391–397.
35. Acevedo, L.M., Barillas, S., Weis, S.M., Gothert, J.R., and Cheresh, D.A. 2008. Semaphorin 3A suppresses VEGF-mediated angiogenesis yet acts as a vascular permeability factor. *Blood.* **111**:2674–2680.
36. De Palma, M., Venneri, M.A., Roca, C., and Naldini, L. 2003. Targeting exogenous genes to tumor angiogenesis by transplantation of genetically modified hematopoietic stem cells. *Nat. Med.* **9**:789–795.
37. Rajantie, I., et al. 2004. Adult bone marrow-derived cells recruited during angiogenesis comprise precursors for periendothelial vascular mural cells. *Blood.* **104**:2084–2086.
38. Song, S., Ewald, A.J., Stallcup, W., Werb, Z., and Bergers, G. 2005. PDGFRbeta+ perivascular progenitor cells in tumours regulate pericyte differentiation and vascular survival. *Nat. Cell Biol.* **7**:870–879.
39. Hirschi, K.K., Rohovsky, S.A., and D'Amore, P.A. 1998. PDGF, TGF-beta, and heterotypic cell-cell interactions mediate endothelial cell-induced recruitment of 10T1/2 cells and their differentiation to a smooth muscle fate. *J. Cell Biol.* **141**:805–814.
40. Leveen, P., et al. 1994. Mice deficient for PDGF B show renal, cardiovascular, and hematological abnormalities. *Genes Dev.* **8**:1875–1887.
41. Suri, C., et al. 1996. Requisite role of angiopoietin-1, a ligand for the TIE2 receptor, during embryonic angiogenesis. *Cell.* **87**:1171–1180.
42. Hirschi, K.K., Rohovsky, S.A., Beck, L.H., Smith, S.R., and D'Amore, P.A. 1999. Endothelial cells modulate the proliferation of mural cell precursors via platelet-derived growth factor-Bb and heterotypic cell contact. *Circ. Res.* **84**:298–305.
43. Heil, M., and Schaper, W. 2004. Influence of mechanical, cellular, and molecular factors on collateral artery growth (arteriogenesis). *Circ. Res.* **95**:449–458.
44. Hoefer, I.E., et al. 2004. Arteriogenesis proceeds via ICAM-1/Mac-1- mediated mechanisms. *Circ. Res.* **94**:1179–1185.
45. Ito, W.D., et al. 1997. Monocyte chemotactic protein-1 increases collateral and peripheral conductance after femoral artery occlusion. *Circ. Res.* **80**:829–837.
46. Strauer, B.E., et al. 2002. Repair of infarcted myo-

cardium by autologous intracoronary mononuclear bone marrow cell transplantation in humans. *Circulation.* **106**:1913–1918.
47. Perin, E.C., et al. 2003. Transendocardial, autologous bone marrow cell transplantation for severe, chronic ischemic heart failure. *Circulation.* **107**:2294–2302.
48. Stamm, C., et al. 2003. Autologous bone-marrow stem-cell transplantation for myocardial regeneration. *Lancet.* **361**:45–46.
49. Perin, E.C., et al. 2004. Improved exercise capacity and ischemia 6 and 12 months after transendocardial injection of autologous bone marrow mononuclear cells for ischemic cardiomyopathy. *Circulation.* **110**:II213–II218.
50. Yaoita, H., et al. 2005. Scintigraphic assessment of the effects of bone marrow-derived mononuclear cell transplantation combined with off-pump coronary artery bypass surgery in patients with ischemic heart disease. *J. Nucl. Med.* **46**:1610–1617.
51. Todorovic, V., et al. 2005. Human origins of DNA replication selected from a library of nascent DNA. *Mol. Cell.* **19**:567–575.
52. Miles, A.A., and Miles, E.M. 1952. Vascular reaction to histamine, histamine-liberator, and leukotaxine in the skin of guinea pigs. *J. Physiol.* **118**:228–257.
53. Elbashir, S.M., Harborth, J., Weber, K., and Tuschl, T. 2002. Analysis of gene function in somatic mammalian cells using small interfering RNAs. *Methods.* **26**:199–213.